



Cite this: *Dalton Trans.*, 2015, **44**, 2517

Received 6th August 2014,
Accepted 18th September 2014

DOI: 10.1039/c4dt02391a

www.rsc.org/dalton

Actinide-based single-molecule magnets

Katie R. Meihaus and Jeffrey R. Long*

Actinide single-molecule magnetism has experienced steady growth over the last five years since the first discovery of slow magnetic relaxation in the mononuclear complex $\text{U}(\text{Ph}_2\text{BPz}_2)_3$. Given their large spin-orbit coupling and the radial extension of the 5f orbitals, the actinides are well-suited for the design of both mononuclear and exchange-coupled molecules, and indeed at least one new system has emerged every year. By some measures, the actinides are already demonstrating promise for one day exceeding the performance characteristics of transition metal and lanthanide complexes. However, much further work is needed to understand the nature of the slow relaxation in mononuclear actinide complexes, as well as the influence of magnetic exchange on slow relaxation in multinuclear species. This perspective seeks to summarize the successes in the field and to address some of the many open questions in this up and coming area of research.

Introduction

The field of single-molecule magnetism has seen tremendous changes since the discovery of slow magnetic relaxation in the transition metal cluster $\text{Mn}_{12}\text{O}_{12}(\text{CH}_3\text{COO})_{16}(\text{H}_2\text{O})_4$.¹ Notably, a significant amount of progress has occurred within the last ten years, concomitant with the observation of the same phenomenon in the lanthanide sandwich complexes $[\text{LnPc}_2]^-$ ($\text{Ln} = \text{Tb}, \text{Dy}$; Pc^{2-} = phthalocyanine dianion).² Thus, while single-molecule magnets were initially thought to be best engineered through magnetic coupling of transition metal centers and the generation of a large spin ground state, the greater magnetic moments and unquenched orbital angular momentum of the lanthanides challenged this notion. Indeed, with only a single lanthanide metal center, higher blocking temperatures have been achieved than with any transition metal system.³ It has also recently been shown that the use of weakly-donating ligands and low coordination numbers in mononuclear transition metal complexes can minimize quenching of orbital angular momentum and maximize anisotropy, in a fashion analogous to lanthanide systems.⁴ Multinuclear systems still continue to hold promise, however, particularly in the light of recent developments with radical bridging ligands, which can promote exceptionally strong exchange in both transition metal⁵ and lanthanide molecules.⁶

The stage was thus set for entrance of the actinides into single-molecule magnetism. Indeed, the spin-orbit coupling of the actinides far exceeds the lanthanides,⁷ and the greater radial extension of the 5f over the 4f orbitals (Fig. 1)⁸

introduces the possibility of covalency and strong magnetic exchange.⁹ Such an opportune melding of the properties of lanthanides and transition metals has led to the actinides being frequently touted as a promising new route to single-molecule magnets with higher blocking temperatures. However, research into this area is still developing, and the systems studied to date have revealed a complexity not yet encountered with 3d or 4f forerunners. Nonetheless, with an increased effort in the design and rigorous characterization of actinide systems, this nascent area has the potential to blossom just as its predecessors did. This perspective aims to provide both a survey of the existing systems as well as a critical examination of the current state of the field, with an eye toward the most successful routes in the future. The reader is also referred to a few excellent recent reviews on lanthanide,¹⁰

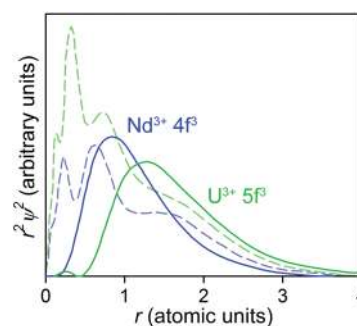


Fig. 1 Radial probability distribution functions for trivalent neodymium and uranium (adapted from ref. 8). Solid blue and green lines represent the probability distributions for the three valence f electrons of Nd^{3+} and U^{3+} , respectively, relative to their core electrons (dashed lines).

Department of Chemistry, University of California, Berkeley, California 94720, USA.
E-mail: jrlong@berkeley.edu; Tel: (+1) 510 642 0860

organometallic,¹¹ and actinide¹² single-molecule magnets for additional details and outlook.

Some general considerations

As already mentioned, the actinides are unique given that in principle they combine the advantageous attributes of both the lanthanides and transition metals. The combination of qualities such as large magnetic anisotropy and the possibility for covalency, however, necessarily adds some new complexity. For instance, while covalency is advantageous for generating strong magnetic exchange, on the other hand it introduces a challenge to the rational design of mononuclear actinide complexes thus far not encountered with the lanthanides. This can be understood when considering that, to date, arguably the most common and successful synthetic rationale in the design of mononuclear lanthanide systems is to choose an appropriate ligand field symmetry such that a maximal M_J ground state electron density distribution is likely to be preferentially stabilized.¹³ One main reason this approach has worked well for the lanthanides is that they do not participate in covalent bonding; therefore their orbital angular momentum remains largely unquenched and the ligand field acts as a minor electrostatic perturbation that splits the degenerate M_J states within the ground J manifold. With the potential for covalency and therefore partial quenching of orbital angular momentum, such an approach for the actinides is less straightforward.¹⁴ Taking a synthetic cue from recent developments in mononuclear transition metal complexes, a promising avenue for future mononuclear actinide systems could be to design low-coordinate complexes of weakly donating ligands, in order to maximize anisotropy. Given the oxophilic nature and large ionic radii of the actinides (~ 0.95 – 1.05 Å for An^{3+}), however, such a goal will no doubt be a formidable synthetic challenge.

On the other hand, one advantage of covalency in actinide complexes may be the resulting larger overall crystal field splitting achieved when compared to isoelectronic lanthanide complexes.^{7,8,15} Table 1 compares values of the spin–orbit coupling interaction (ζ_{nf}), crystal field splitting, and B_0^2 crystal field parameter for two different compounds of U^{3+} and Nd^{3+} , obtained from parametric analysis of absorption and fluorescence spectra.¹⁶ Both the spin–orbit coupling and crystal

field parameters are nearly double for both uranium systems in comparison with their Nd^{3+} analogues. Accompanying a larger crystal field splitting is a larger magnitude for B_0^2 , which influences the sign and magnitude of the overall magnetocrystalline anisotropy.¹⁷ In turn, the larger crystal field also yields a larger separation between ground and first excited M_J states. Thus, much larger barriers and preferential Orbach relaxation might be accessible for the actinides compared to the lanthanides.^{13a,b} This reasoning also suggests that the study of isoelectronic lanthanide complexes may provide a simple first pass in order to decipher potentially interesting actinide systems, especially for more challenging transuranic elements. For instance, when the study of an f^1 or f^3 actinide system is of interest, an isostructural Ce^{III} or Nd^{III} complex may serve as a good model.

The remarkable range of oxidation states accessible among the actinides is another potentially promising peculiarity. For instance, uranium is synthetically accessible in oxidation states ranging from +3 to +6, and even very recently +2.¹⁸ Even considering only Kramers ions ($S = \text{half integer}$), which are guaranteed to possess a doubly-degenerate $\pm M_J$ ground state in the absence of an applied field, then for the first half of the actinides there are twice as many potential magnetic centers as for the lanthanides. The very obvious caveat here is that this seeming abundance of choices is seriously limited by the accessibility and practicality of studying certain actinides. Only a handful of institutions in the world are equipped with all the means necessary to study transuranic single-molecule magnets, and the latter half of the 5f elements is perhaps entirely impractical due to the limitations of short half-lives and self heating. Not surprisingly, then, the study of slow relaxation among the actinides is dominated by the relatively stable and abundant ²³⁸U isotope. However, as discussed below, neptunium appears to be quite promising in both mono- and multinuclear complexes. Thus, for an ambitious few, the first half of the series presents a fundamentally fascinating and exotic playground for molecular magnetism.

Mononuclear and dinuclear complexes

All but three of the known mono- or dinuclear actinide single-molecule magnets are based on uranium(III), a Kramers ion with a large total angular momentum ground state ($5f^3$, $J = 9/2$). The other systems are known with Np^{IV} (also $5f^3$), U^{V} ($5f^1$, $J = 5/2$), and Pu^{III} ($5f^5$, $J = 5/2$). Mononuclear complexes in particular are ideal for developing a more fundamental understanding of slow relaxation among the actinides, as these systems can be rationally designed and the absence of magnetic exchange simplifies computational modelling.

Complexes of uranium(III)

The first actinide system found to display slow magnetic relaxation was the mononuclear complex $\text{U}(\text{Ph}_2\text{BPz}_2)_3$.¹⁹ This molecule had been synthesized ten years earlier and found to possess a trigonal prismatic geometry arising from the coordi-

Table 1 Comparison of spin–orbit coupling and crystal field splitting for isoelectronic U^{3+} and Nd^{3+} compounds; all values are reported in cm^{-1} ^a

Complex	ζ_{nf}	$N_f/\sqrt{4\pi}^b$	E (1 st excited M_J)	B_0^2
$\text{LaCl}_3:\text{U}^{3+}$	1607	634	208	260(64)
$\text{LaCl}_3:\text{Nd}^{3+}$	880	300	115	163
UTp_3	1516	1386	270	–1124
NdTp_3	881	514	107	–512

^a All values obtained from ref. 8,15 and references therein. ^b Measure of crystal field strength.

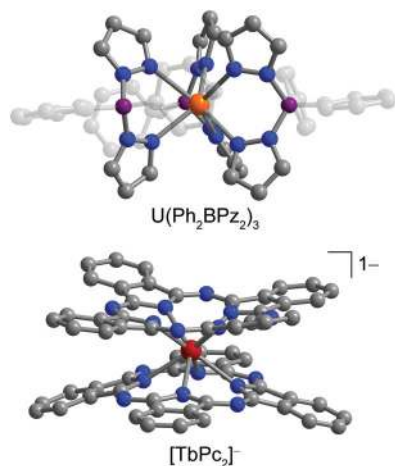


Fig. 2 Molecular structures of the first actinide and lanthanide single-molecule magnets U(Ph₂BPz₂)₃ (top)¹⁹ and [TbPc₂]⁻ (bottom)², respectively. Red, orange, blue, purple, and grey spheres represent Tb, U, N, B, and C atoms, respectively; H atoms are omitted for clarity.

nation of three bidentate diphenyl(bispyrazolyl)borate ligands (Fig. 2).²⁰ The realization of slow relaxation in this complex was not serendipitous, however. Indeed, it was observed that the N donor atoms above and below the plane of the uranium center should present an axial ligand field somewhat analogous to that of the phthalocyanine sandwich complexes [LnPc₂]⁻ (Fig. 2).² Given that U³⁺ possesses a ground $J = 9/2$ with oblate-type anisotropy akin to the highly anisotropic Tb³⁺ and Dy³⁺ ions,^{13a} it was reasoned that this axial donor set could potentially provide an effective strategy for engineering slow magnetic relaxation. Indeed, this complex was found to relax slowly under zero applied field with a thermally-activated relaxation barrier of 20 cm⁻¹ and $\tau_0 = 1 \times 10^{-7}$ s. While the U_{eff} value was more than an order of magnitude smaller than record lanthanide barriers at the time, this result opened up a new area of molecular magnetism based upon actinide ions.

Subsequent studies sought to discern how slight electronic changes made *via* modifications to the ligands might influence relaxation behavior at the uranium center. By replacing the ancillary phenyl groups with hydrogen atoms, one obtains the complex U(H₂BPz₂)₃.²¹ Interestingly, one hydrogen from each boron center interacts agostically with the uranium, as confirmed by infrared spectroscopy. This interaction leads to a tricapped trigonal prismatic coordination geometry, wherein the trigonal prism of U(H₂BPz₂)₃ is elongated relative to U(Ph₂BPz₂)₃ due to the presence of equatorial electron density around the uranium center. This axial elongation was originally given as rationale for the much smaller experimental barrier of 8 cm⁻¹ for this complex, observed only under an applied dc field.²²

Intriguingly, for fields larger than 500 Oe, U(H₂BPz₂)₃ also displayed a second relaxation process, evident as a second Cole–Cole semicircle in the frequency range 1–1500 Hz (Fig. 3, blue circles). While initially assumed to be molecular in origin, measurements on magnetically dilute samples of

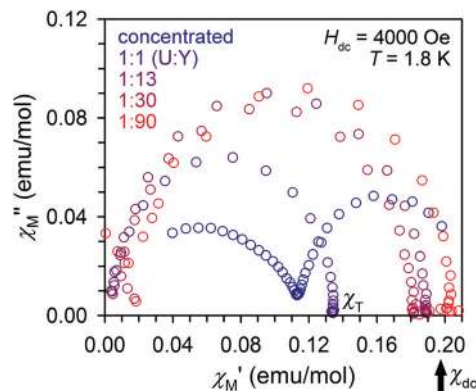


Fig. 3 Cole–Cole plots collected at 1.8 K and under an applied field of 4000 Oe for increasing magnetic dilutions of U(H₂BPz₂)₃ in a matrix of Y(H₂BPz₂)₃. Blue circles correspond to data for the pure compound U(H₂BPz₂)₃, for which two distinct relaxation processes occur in the ac frequency range 0.1–1500 Hz (right to left). With increasing dilution, the low frequency process moves first out of the ac time-scale (purple circles, 1 : 1 dilution) and eventually is extinguished entirely (red circles, 1 : 90 (U : Y) dilution). When all relaxation processes are accounted for, the isothermal susceptibility value χ_T agrees with the static susceptibility χ_{dc} value at the same temperature.²³

U(H₂BPz₂)₃ within a matrix of Y(H₂BPz₂)₃ revealed this second process to derive from intermolecular interactions. Indeed, for a molar dilution of 1 : 90 (U : Y) this second process was completely extinguished. The significant impact of magnetic dilution on this second relaxation process can be visualized by overlaying the isothermal Cole–Cole plots for the various magnetic dilutions under an applied field of 4000 Oe (Fig. 3). Notably, for a 1 : 1 (U : Y) molar ratio the intermolecular relaxation process is no longer observed in the Cole–Cole plot; however the discrepancy between χ_T (the isothermal susceptibility) and χ_{dc} for this dilution indicated that a portion of the total magnetic susceptibility was not being accounted for on the ac timescale probed. Indeed, variable field magnetization measurements at low temperature revealed this intermolecular process was still active, though slowed significantly such that butterfly magnetic hysteresis could be observed as high as 3 K. A final consequence of dilution in this system was to increase molecular thermal relaxation times, leading to a doubling of the thermally-activated barrier to 16 cm⁻¹ for a 1 : 90 dilution.²³

A recent computational investigation using a corrected crystal field model²⁴ was carried out on U(Ph₂BPz₂)₃ and U(H₂BPz₂)₃ to determine the wave functions and sublevel splitting of the ground $J = 9/2$ state. While this method predicts comparable ground to first excited state separations for the two complexes, the values are 190 and 230 cm⁻¹ respectively, a shocking order of magnitude larger than the experimental U_{eff} values. This experimental and computational mismatch is the rule and not the exception for mononuclear actinide single-molecule magnets. For instance, the field-induced single-molecule magnet UTP₃ presents the most extreme case of this discrepancy, as both spectroscopic and crystal field approaches predict a relaxation barrier of $U \sim 270$ cm⁻¹ assuming relaxation through the first excited state, while the experimental

Table 2 Actinide single-molecule magnets (and one single-chain magnet) along with relevant diagnostic parameters

Complex	U_{eff}^a (cm ⁻¹)	U_{calc} (cm ⁻¹)	τ_0 (s)	Crystal symmetry	Hysteresis ^f (K)	χ_T matches χ_{dc}^{2h}	Ref.
U(Ph ₂ BPz ₂) ₃	20	190	1×10^{-7} ^e	$P\bar{1}$		Too large	19
U(H ₂ BPz ₂) ₃	16	230	4×10^{-7}	$C2/c$	3 ^g	Yes	22,23
UTp ₃	3.8	270	7×10^{-5}	$P6_3/m$		Too large	25
[UTp ^{Me2} ₂ (bipy)]I	18.2	137 ^c	1.4×10^{-7}	$C2/c$	0.32	Yes	27
[UTp ^{Me2} ₂ (bipy)]	19.8 ^b		3.28×10^{-7}	$P2_1/c$	0.8	Yes	31
[UTp ^{Me2} ₂]I	21.0	187 ^d	1.8×10^{-7}	$C2/m$	3	Too large	28,29
UI ₃ (THF) ₄	12.9		6.4×10^{-7}	$P2_1/c$		Too large	32
U[N(SiMe ₃) ₂] ₃	22		10^{-11}	$P\bar{3}_1c$		Too large	32
[U(BIPM ^{TMS})(I ₂)(THF)]	16.3		2.9×10^{-7}	$P\bar{1}$		Too large	32
U(Bc ^{Me}) ₃	23		1×10^{-7}	$R\bar{3}$		Yes	26
U(Bp ^{Me}) ₃				$R\bar{3}$		Yes	26
[U(BIPM ^{TMS})I] ₂ (μ-C ₆ H ₅ CH ₃)				$Fdd2$	1.8		33
UO(Tren ^{TIPS})	14.9		2.6×10^{-7}	$P2_1/c$	2.4	Yes	34
{[UO ₂ (salen)] ₂ Mn(Py) ₃ } ₆	98.7		3×10^{-12}		4		58a
[UO ₂ (salen)(Py)][Mn(Py) ₄](NO ₃)	93		3.1×10^{-11}		3		58b
Np(COT) ₂	28.5	1400	1.1×10^{-5}	$P2_1/n$	1.8		35
(Np ^{VI} O ₂ Cl ₂)[Np ^V O ₂ Cl(THF) ₃] ₂	97		not reported				9
PuTp ₃	18.3	332	2.9×10^{-7}	$P6_3/m$		Too large	38

^a Obtained under H_{dc} except for U(Ph₂BPz₂)₃, [UTp^{Me2}₂(bipy)], {[UO₂(salen)]₂Mn(Py)₃}₆, [UO₂(salen)(Py)][Mn(Py)₄](NO₃), and (Np^{VI}O₂Cl₂)[Np^VO₂Cl(THF)₃]₂. ^b Under zero dc field; under 500 Oe the barrier increases to 22.6 cm⁻¹ with $\tau_0 = 4.68 \times 10^{-8}$ s. ^c Average of the values calculated from SO-CASPT2 method and a corrected crystal field model (136 cm⁻¹ and 138 cm⁻¹, respectively). ^d Determined from the SO-CASPT2 method performed on the high-symmetry cationic structure, see ref. 29. ^e The previously reported τ_0 value was 1×10^{-9} s; however re-plotting of the data revealed this to be an error, with the actual value equal to 1×10^{-7} s. ^f Maximum reported hysteresis temperature. ^g Hysteresis due to intermolecular interactions. ^h See ref. 44.

“barrier” is nearly two orders of magnitude smaller at 3.8 cm⁻¹ (Table 2).²⁵

Given the predominance of N-donor scorpionate ligands, it became of interest to study how changing the donor atom within the same molecular symmetry might influence relaxation behavior. A comparison of slow magnetic relaxation in the isostructural scorpionate complexes U(Bc^{Me})₃ ([Bc^{Me}]⁻ = dihydrobis(methylimidazolyl)borate anion) and U(Bp^{Me})₃ ([Bp^{Me}]⁻ = dihydrobis(methylpyrazolyl)borate anion) revealed that the more strongly-donating N-heterocyclic carbene engineers slower relaxation under an applied magnetic field with a much greater thermal dependence (Fig. 4).²⁶ Simulation of low

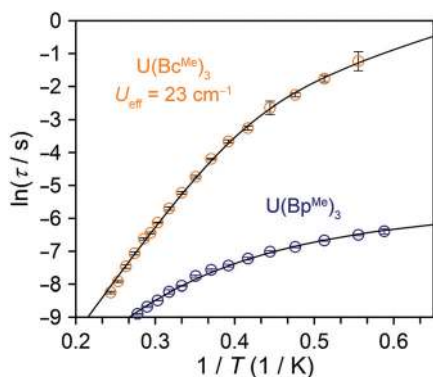


Fig. 4 Plot of $\ln(\tau)$ versus $1/T$ for magnetically dilute samples of 12 mol% U(Bc^{Me})₃ (orange circles) and 11 mol% U(Bp^{Me})₃ (blue circles) in the corresponding isostructural Y^{III} complex. Black lines represent fits to the equation $\tau^{-1} = AT^m + \tau_0^{-1} \exp(-U_{\text{eff}}/k_B T) + CT^n$ accounting for direct, Orbach, and Raman spin-lattice relaxation processes, respectively. Through fitting with this equation, only U(Bc^{Me})₃ was determined to relax through a thermally-activated process at high temperatures.²⁶

temperature X-band EPR data revealed the ground state to be similar in both complexes, though the N-heterocyclic carbene donor species is more magnetically anisotropic, providing some rationale for its slower relaxation behavior. Even still, the apparent thermally activated experimental barrier for magnetically dilute U(Bc^{Me})₃ was only 23 cm⁻¹, notably very close to those determined for U(Ph₂BPz₂)₃ and U(H₂BPz₂)₃. While no computational studies have been done on U(Bc^{Me})₃ or U(Bp^{Me})₃, it is tempting to conjecture that a similar discrepancy between calculated and experimental relaxation barriers will also be encountered for these systems.

Two additional scorpionate-based complexes [UTp^{Me2}₂(bipy)]I²⁷ ([Tp^{Me2}]⁻ = hydrotris(dimethylpyrazolyl)borate anion, bipy = 2,2'-bipyridine) and [UTp^{Me2}₂]I^{28,29} were shown to relax slowly in the presence of a small dc field, with experimental relaxation barriers of 18.2 and 21.0 cm⁻¹, respectively. Following the same trend as above, these values are only a fraction of the calculated ground to first excited state gaps determined using the aforementioned crystal field approach or *ab initio* methods (Table 2). Notably, the 2,2'-bipyridine radical complex [UTp^{Me2}₂(bipy)],³⁰ obtained from reduction of [UTp^{Me2}₂(bipy)]I with sodium amalgam, was found to relax slowly under zero dc field, with $U_{\text{eff}} = 19.8$ cm⁻¹.³¹ This result is a promising indication that magnetic coupling can efficiently diminish tunnelling of the magnetization even in mononuclear uranium complexes. For all three of the above complexes, magnetic hysteresis could furthermore be observed at low temperatures. While [UTp^{Me2}₂(bipy)]I and [UTp^{Me2}₂(bipy)] show hysteresis only below 1 K, [UTp^{Me2}₂]I presents a butterfly hysteresis loop as high as 3 K.

Three additional mononuclear complexes with more diverse ligand sets have also been shown to relax slowly in the presence of a dc field. The compounds UI₃(THF)₄,

$U[N(\text{SiMe}_3)_2]_3$, and $[U(\text{BIPM}^{\text{TMS}})(\text{I}_2)\text{THF}]$ ($\text{BIPM}^{\text{TMS}} = \text{CH}[\text{PPh}_2\text{NSiMe}_3]_2$) present remarkably similar relaxation with barriers of 12.9, 22, and 16.2 cm^{-1} , respectively, despite their different symmetries. Although no calculated energy barriers are available for these complexes, the experimental values are small and similar to those reported for scorpionate-based systems. No magnetic hysteresis was observed for these samples. While solution measurements confirmed the molecular origins of the slow magnetic relaxation, the values of U_{eff} were smaller than determined for the concentrated species.³²

Another U^{3+} complex reported to show slow magnetic relaxation under a dc field of 0.1 T is the dinuclear arene-bridged species $[U(\text{BIPM}^{\text{TMS}})\text{I}]_2(\mu\text{-C}_6\text{H}_5\text{CH}_3)$.³³ The observed relaxation was very fast, however, such that peaks in the out-of-phase susceptibility were only apparent below 3 K and at high frequencies of the oscillating field, precluding the extraction of relaxation times. In spite of estimated ac relaxation times on the order of a few milliseconds, a butterfly-shaped magnetic hysteresis loop was also reported for this complex at 1.8 K.

Complexes of uranium(v), neptunium(iv), and Pu(III)

Three additional mononuclear systems illustrate the diversity accessible with actinide single-molecule magnets. The first of these is the C_{3v} symmetric uranium(v) complex $\text{UO}(\text{Tren}^{\text{TIPS}})$ ($\text{Tren}^{\text{TIPS}} = [\text{N}(\text{CH}_2\text{CH}_2\text{NSi}^i\text{Pr}_3)_3]^{3-}$), for which a pure $M_J = \pm 3/2$ ground state was inferred from magnetization and EPR studies.³⁴ Slow magnetic relaxation was observed for this complex only under an applied dc field, with a relaxation barrier of 14.9 cm^{-1} , the same order of magnitude as observed for mononuclear U^{III} complexes. Despite a very small relaxation barrier, this U^{V} complex was also reported to show butterfly-shaped magnetic hysteresis loops as high as 2.4 K.

One of only two mononuclear transuranic systems displaying slow magnetic relaxation is the homoleptic bis(cyclooctatetraenide) complex $\text{Np}(\text{COT})_2$, as probed under applied fields greater than 0.1 T.³⁵ Notably, earlier characterization of this complex at 4.2 K using Mössbauer spectroscopy revealed magnetic splitting of the quadrupole doublet, which was attributed to the occurrence of slow spin-lattice relaxation.³⁶ A rigorous ligand field analysis estimated the ground state of this complex to be predominantly $M_J = \pm 5/2$, separated from the first excited state by an enormous energy gap of $\sim 1400 \text{ cm}^{-1}$. However, under an applied field of 0.3 T, an energy barrier of just 28.5 cm^{-1} was determined. Under larger applied fields ($> 5 \text{ T}$), it was found that the relaxation times for this complex slow dramatically, leading to very steep Arrhenius behavior and the opening of a magnetic hysteresis loop above 5 T at 1.8 K. The fast relaxation at low fields was attributed to hyperfine interactions of the $M_J = \pm 5/2$ ground doublet with the $I = 5/2$ nuclear spin of ^{237}Np .³⁷

Very recently, PuTp_3 was reported to show slow magnetic relaxation under a dc field of 100 Oe ($H_{\text{ac}} = 10 \text{ Oe}$) and to temperatures as high as 12 K, with $U_{\text{eff}} = 18.3 \text{ cm}^{-1}$. This compound represents the first plutonium-based single-molecule magnet, and possesses the same symmetry as its U^{3+} congener. Accordingly, by using the same crystal field parameters as those

obtained spectroscopically for UTp_3 (ref. 15b), the authors were able to extract wave functions and energies of the sublevels within the ground $J = 5/2$ manifold. The ground state is predominantly $M_J = \pm 5/2$ and separated from a nearly pure excited $M_J = \pm 3/2$ by 332 cm^{-1} , almost 20 times that of the experimental barrier. The authors note that the relaxation mechanism is therefore more complex than for transition metal clusters (and we add here, also many lanthanide complexes).³⁸

Fast relaxation and U_{eff} discrepancies

From the above survey, two distinct trends distinguish low-nuclearity actinide single-molecule magnets from their 4f predecessors. The first is the very small (and remarkably similar) U_{eff} values across all compounds, when available calculations predict much larger separations between the ground and first excited state M_J doublets. This difference is illustrated for $[\text{UTp}^{\text{Me}_2}]$ and $[\text{UTp}^{\text{Me}_2}(\text{bipy})]$ in the top panel of Fig. 5, and is in contrast to many lanthanide complexes, wherein U_{eff} values have been found to correlate with the ground to first excited state energy gap.^{2,39}

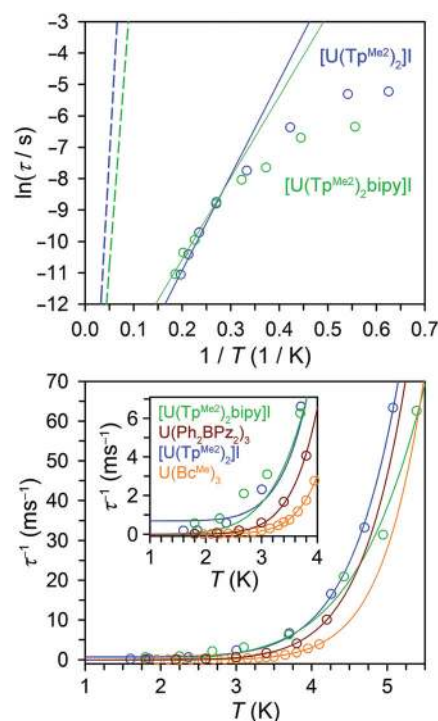


Fig. 5 (Top) Plot of $\ln(\tau)$ versus $1/T$ for $[\text{UTp}^{\text{Me}_2}]$ and $[\text{UTp}^{\text{Me}_2}(\text{bipy})]$ ($H_{\text{dc}} = 500 \text{ Oe}$). Circles represent experimental data, solid lines represent linear Arrhenius fits, and dashed lines represent the predicted Arrhenius behavior assuming calculated ground to first excited M_J separations of 187 cm^{-1} and 138 cm^{-1} , respectively, and a τ_0 of $1 \times 10^{-9} \text{ s}$. (Bottom) Plot of the inverse relaxation time versus T for $[\text{UTp}^{\text{Me}_2}]$, $[\text{UTp}^{\text{Me}_2}(\text{bipy})]$, $\text{U}(\text{Bc}^{\text{Me}})_3$, and $\text{U}(\text{Ph}_2\text{BPz})_3$. Circles represent the full range of temperature-dependent data and solid lines represent fits to a Raman relaxation process. Values of C/n were found to be 0.15(7)/7.9(2); 2(1)/6.2(5); 0.002(6)/9.91(1); and 0.034(8)/8.8(2) for each complex, respectively. In the case of $[\text{UTp}^{\text{Me}_2}]$ the fit was improved by also accounting for quantum tunnelling of the magnetization with $\tau_{\text{QTM}} = 1.5(9) \text{ ms}$. (Inset) Expanded view of the low temperature fit region.^{19,26–29}

For $\text{Np}(\text{COT})_2$ the mismatch cannot be explained by hyperfine interactions, for even under large dc fields where these should be irrelevant, the experimental barrier is still only a fraction of the calculated value. For the uranium systems, the scenario is even more opaque. While ^{238}U has no nuclear spin, dipolar interactions may play a role in speeding up molecular relaxation, though measurements on magnetically dilute actinide molecules are sparse. Assuming the predicted relaxation barriers are correct in their order of magnitude estimate, it appears that the relaxation observed on the ac timescale must necessarily be some other spin-lattice relaxation process that is not truly thermally-activated.

With this in mind, we thought it illustrative to plot the inverse of the relaxation time, τ^{-1} , versus temperature for some of the aforementioned complexes, to gain insight into the relevance of Raman or direct processes. Interestingly, the whole range of temperature-dependent data for $[\text{UTp}^{\text{Me}_2}_2]\text{I}$ and $[\text{UTp}^{\text{Me}_2}_2(\text{bipy})]\text{I}$ can be fit quite well to a power dependence on temperature, *i.e.* $\tau^{-1} = CT^n$, corresponding to a two-phonon Raman process.⁴⁰ The same procedure also provides very good fits for $\text{U}(\text{Ph}_2\text{BPz}_2)_3$ and $\text{U}(\text{Bc}^{\text{Me}})_3$ (Fig. 5, lower). Thus, in the characterization of future systems it will be important to evaluate the temperature-dependent relaxation data for all relevant relaxation processes in order to determine which is the most reasonable. At this point of course, the lingering question remains as to why Orbach relaxation seems largely inaccessible in these systems.

One possible culprit is that for all of the mononuclear compounds discussed above, the ground M_J is non-maximal.⁴¹ Such a scenario is less than ideal, as a maximal M_J ground state corresponds to the largest projection of the angular momentum and therefore the greatest magnetic anisotropy. In the case of the homoleptic scorpionate systems, the ground state is also impure, due to symmetry-allowed mixing between $M_J = \pm 5/2$ and $M_J = \pm 7/2$.⁴² This result derives from the presence of approximate C_{3h} or D_{3h} symmetry for most of these complexes,⁴³ which will always allow mixing of M_J states that differ by ± 6 due to the B_6 crystal field parameter.^{26,44} It may thus seem ideal to move away from ligands that enforce a trigonal prismatic geometry in pursuit of larger magnitude ground states. However, as has been previously addressed in ref. 24, the solution is not so simple, for instance in tetragonal symmetry the ground state will likely be of larger magnitude $M_J = \pm 9/2$ or $M_J = \pm 7/2$, though there will be heavy symmetry-allowed mixing with $M_J = \pm 1/2$.²⁴ One remedy is perhaps to move toward systems with much higher symmetry, such as D_{5h} or $C_{\infty v}$, wherein mixing of states will be less facile due to the reduction in crystal field parameters.^{3a} Either of these approaches would present non-trivial synthetic challenges, however.⁴⁵ Ultimately, a more rigorous understanding of the relationship between the temperature-dependent relaxation and the magnetic ground state will surely require more exotic experimental methods and computational analysis. Such an investigation will certainly be worthwhile toward informing future synthetic designs.

Magnetic hysteresis and dipolar interactions

The second trend for the foregoing complexes is the existence of magnetic hysteresis at low temperatures. The pervasive assumption here is that this hysteresis is due to molecular relaxation; however only for $\text{U}(\text{H}_2\text{BPz}_2)_3$ was the origin of magnetic hysteresis thoroughly vetted and found to arise from intermolecular interactions, even at a separation of ~ 8.5 Å (importantly, this relaxation process is strongly field-dependent, and grows in magnitude with increasing applied fields). Therefore, the common logic that a separation of ~ 8 – 9 Å should preclude strong dipolar interactions is not wholly founded. Indeed, even with an average intermolecular spacing of >11 Å for a 1 : 13 (U : Y) dilution of $\text{U}(\text{H}_2\text{BPz}_2)_3$, a narrow butterfly-shaped hysteresis loop was still observed at 1.8 K.²³

In fact, before attempting the study of dilute samples, a very simple check can be performed to determine whether dipolar relaxation (in the form of fast or slow processes) deserves further attention. This check is to compare the isothermal susceptibility value (χ_T) with the static magnetic susceptibility value at the same temperature (χ_{dc}). If the ac relaxation process under study represents the predominant one, then these two susceptibility values should agree for a given temperature and range of magnetic fields. If instead χ_T is less than χ_{dc} , this suggests a slower relaxation process is also occurring, and perhaps dipolar interactions could play a role.⁴⁶ Without variable-field data for most of the compounds under consideration here, it is impossible to say whether dipolar interactions are important in the relaxation and observed magnetic hysteresis. However, as the following analysis suggests, the molecular origins of magnetic hysteresis are not necessarily definitive, and it seems important that dipolar interactions and the possibility of additional relaxation mechanisms be considered for these and future low-nuclearity systems.

Consider the example of $\text{Np}(\text{COT})_2$, which shows very slow low-temperature relaxation for applied fields greater than 5 T, and an open magnetic hysteresis loop above this field. While the provided linear fit of the 7 T Arrhenius data gives a large barrier to magnetic relaxation of ~ 471 cm⁻¹, the corresponding τ_0 value is shockingly small, at $\sim 7 \times 10^{-19}$ s (Fig. 6). Such a small value is typically not associated with slowly-relaxing molecular species but rather relaxation in spin glasses, and it can often be challenging to distinguish the two.⁴⁷ Spin glasses are furthermore often characterized by magnetic hysteresis loops that fail to show saturation and exhibit an out-of-phase signal with little frequency dependence. Both of these are characteristics displayed by $\text{Np}(\text{COT})_2$ under large applied fields. For a field of 5 T, the low temperature relaxation time spikes below ~ 11 K and, as the authors note, becomes frequency-independent. Thus, it appears that for the relaxation under large applied fields, and therefore also the magnetic hysteresis, the possibility of relaxation processes beyond molecular spin-lattice pathways must be addressed.

A similar analysis can be accomplished for $[\text{UTp}^{\text{Me}_2}_2]\text{I}$. From the Arrhenius data reported at 500 Oe, it is apparent that below ~ 3.5 K, the relaxation tends away from thermally acti-

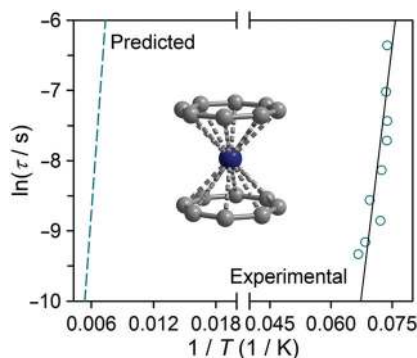


Fig. 6 Plot of $\ln(\tau)$ versus $1/T$ for $\text{Np}(\text{COT})_2$ (molecular structure inset) under $H_{\text{dc}} = 7 \text{ T}$.³⁵ Circles represent experimental data and the solid line represents a linear fit to an Arrhenius law, giving $U_{\text{eff}} = 471 \text{ cm}^{-1}$ and $\tau_0 = 7 \times 10^{-19} \text{ s}$. The dashed cyan line represents the predicted Arrhenius behavior assuming a calculated ground to first excited energy splitting of 1400 cm^{-1} and $\tau_0 = 1 \times 10^{-9} \text{ s}$.

ated behavior and becomes temperature-independent. Extrapolating the given Arrhenius parameters ($U_{\text{eff}} = 21.0 \text{ cm}^{-1}$ and $\tau_0 = 4.3 \times 10^{-8} \text{ s}$ ⁴⁸), the relaxation time at 2 K is only 0.18 s, seemingly too fast to allow for the observation of magnetic hysteresis. The one caveat is that the opening of the hysteresis loop for this compound occurs at $\sim 1 \text{ T}$, and ac relaxation data is not provided for this field. However, in the absence of hyperfine interactions or other fast relaxation processes at lower fields, it seems unlikely that the temperature-dependent relaxation at 0.05 T should differ significantly from that measured under a 1 T field. Even if increasing the field lengthens the low-temperature relaxation, it should still follow the determined Arrhenius law, and one should not expect to see hysteresis. This obvious discrepancy seemingly arises from two implicit assumptions: (i) there is no additional fast relaxation process that would significantly speed up the relaxation at fields below 1 T and (ii) the measured temperature-dependent relaxation data is truly representative of relaxation between M_J states. For the first point, a simple dilution can be performed to rule out any fast molecular relaxation due to dipolar fields.

In the second case, we know already that the observed temperature-dependent relaxation in all of these systems deviates significantly from what is expected based on the splitting within the ground J state. If the hysteresis is molecular, however, temperature-dependent relaxation data collected at 1 T might more closely represent the calculated M_J separation for this species, or at least show a dramatic lengthening of τ . Therefore, the measurement of temperature-dependent relaxation data at 1 T should reflect this slower relaxation and the Arrhenius behavior should change dramatically. If instead, the Arrhenius data at 1 T follows the curvature of that at 0.05 T, then this is evidence that the hysteresis is extra-molecular. Thus, with only a few simple additional experiments, it would be possible to obtain a more thorough understanding of the relaxation dynamics in this system.

The same unanswered questions arise upon closer analysis of all the complexes discussed above, and in many cases a few

simple additional experiments could offer much more clarity. The mononuclear actinide complexes already appear in some ways to behave differently than their lanthanide analogues, and thus at such an early point in their research, a more thorough and thoughtful analysis of relaxation behavior is essential. This should involve not only careful choice of characterization measurements, but a thorough analysis of the purity and form of complexes under study.²⁹ Only in this way can we hope that the systems under investigation now will inform us in a productive manner towards future studies.⁴⁹

Slow magnetic relaxation and exchange in multinuclear complexes

The most successful approach thus far in the design of actinide single-molecule magnets has arisen through the study of exchange-coupled systems. Magnetic exchange in actinide complexes has been known for over 20 years, since it was first observed in the dinuclear U^{V} species $[(\text{MeC}_5\text{H}_4)_3\text{U}]_2(\mu\text{-}1,4\text{-N}_2\text{C}_6\text{H}_4)$.⁵⁰ Even before the discovery of slow magnetic relaxation in $\text{U}(\text{Ph}_2\text{BPz}_2)_3$, exchange coupling was recognized as a potential route toward the design of actinide single-molecule magnets.^{51,52} Indeed, exchange constants estimated for complexes such as $[(\text{MeC}_5\text{H}_4)_3\text{U}]_2(\mu\text{-}1,4\text{-N}_2\text{C}_6\text{H}_4)$ ($J = 19(1) \text{ cm}^{-1}$), $(\text{cyclam})\text{Co}[(\mu\text{-Cl})\text{U}(\text{Me}_2\text{Pz})_4]_2$ ($15 \text{ cm}^{-1} \geq J \geq 48 \text{ cm}^{-1}$),⁵³ and the arene-bridged uranium(IV) complex $\text{U}[\text{HC}(\text{SiMe}_2\text{Ar})_2(\text{SiMe}_2\text{-}\mu\text{-N})](\mu\text{-Ar})\text{U}(\text{Ts}^{\text{Xy}})$ ⁵⁴ ($J = 20 \text{ cm}^{-1}$) rival coupling strengths in transition metal complexes, and are the same order of magnitude as the strong lanthanide-radical exchange observed in $[[\{(\text{Me}_3\text{Si})_2\text{N}\}_2(\text{THF})\text{Tb}\}_2(\mu\text{-N}_2)]^-$, the single-molecule magnet exhibiting the highest known blocking temperature.^{6b}

At the same time, strong magnetic exchange is not a necessary prerequisite for the observation of slow magnetic relaxation. For instance, magnetic exchange has been successfully demonstrated in a number of dinuclear lanthanide single-molecule magnets, though the bridging species are predominantly diamagnetic, and the coupling is therefore very weak.⁵⁵ For most of these complexes, furthermore, slow relaxation originates from a single lanthanide ion, and in fact sometimes the weak coupling can even hamper this relaxation due to closely-spaced exchange coupled states that facilitate fast quantum relaxation.⁵⁵ Thus, strong exchange is crucial for achieving a well-isolated ground state, and thereby favouring the observation of slow magnetic relaxation. Indeed, only in the case of $[[\{(\text{Me}_3\text{Si})_2\text{N}\}_2(\text{THF})\text{Ln}\}_2(\mu\text{-}\eta^2\text{-}\eta^2\text{-N}_2)]^-$ has very strong magnetic exchange been demonstrated to be essential to the observed relaxation.^{6a,56} The nature of magnetic exchange is also of significant import, as suggested by recent DFT and *ab initio* calculations on these N_2^{3-} radical-bridged complexes. The calculations predict strong antiferromagnetic coupling for $\text{Ln} = \text{Tb}$, Dy , and Ho^{III} , but ferromagnetic coupling for $\text{Ln} = \text{Er}^{\text{III}}$, an interesting result given that the Er^{III} congener requires an applied field to observe slow relaxation on the ac time-scale, and displays the smallest relaxation barrier.

Ultimately, however, these results suggest that slow magnetic relaxation should be accessible in multinuclear actinide complexes with an appropriate superexchange pathway.

Cation–cation interactions and strong magnetic exchange

A well-established route to superexchange in actinide-containing multinuclear species is through cation–cation interactions, whereby the oxo-ligands of an actinyl unit (commonly uranyl(v)) interact with another metal center. This linkage effectively forms an oxo-bridge between metal centers and to date has been the most successful strategy toward strong coupling between U^V centers⁵⁷ and between U^V and transition metal⁵⁸ or lanthanide centers.⁵⁹

Perhaps not surprisingly, then, the first multinuclear actinide complex to demonstrate both superexchange and slow magnetic relaxation was assembled through cation–cation interactions. The complex $(Np^{VI}O_2Cl_2)[Np^{V}O_2Cl(THF)_3]_2$ is a triangular cluster made up of two chloride-bridged neptunyl(v) units at the base and a capping neptunyl(vi) unit (Fig. 7). Considering the environment of the individual neptunyl moieties, it was found that all three neptunium centers experience a dominant axial ligand field due to strong, short, and nearly linear Np–O bonds. Static magnetic susceptibility measurements on the trinuclear complex revealed a rise in the magnetic susceptibility below 25 K and 3 T, which was attributed

to exchange coupling. This data could be fit by accounting for the strong axial ligand field and also superexchange between neptunyl centers. Coupling between Np^V and Np^{VI} was found to be quite strong with $J = 7.51 \text{ cm}^{-1}$, while only very weak coupling occurs between Np^V centers, with $J = 0.39 \text{ cm}^{-1}$.⁹

In addition to strong exchange, slow magnetic relaxation was observed for this complex under zero applied dc field and a 15 Oe ac field. The temperature-dependent relaxation behavior is approximated well by an Arrhenius law with $U_{\text{eff}} = 97 \text{ cm}^{-1}$ and lacks the marked deviation at low temperature demonstrated by the mononuclear complexes discussed above. Interestingly, the authors noted that the calculated energy gap corresponds well to the presence of an excited $M_J = \pm 5/2$ state of Np^{VI} , which would suggest that the slow magnetic relaxation originates from a single ion, and further exposes the potential promise in designing mononuclear complexes of Np^{VI} with dominant axial ligand fields.

The second actinide-based cluster to demonstrate magnetic exchange and slow magnetic relaxation was also assembled through cation–cation interactions, this time between uranyl(v) moieties and Mn^{II} centers.^{58a} The large, wheel-shaped cluster $\{[UO_2(salen)]_2Mn(Py)_3\}_6$ (Py = pyridine) depicted in Fig. 7 was synthesized from the reaction of $[Cp^*Co][UO_2(salen)(Py)]$ ($[Cp^*]^-$ = decamethylcyclopentadiene anion) and $Mn(NO_3)_2$ in pyridine, in a 2 : 1 ratio. This molecule is structurally unique in that it is the largest actinide-based multinuclear complex and the first to be assembled through UO_2^+ and Mn^{II} interactions. Additionally, the nature of the early metal cation was essential to the formation of such a high nuclearity complex, as the use of Ca^{II} was found to produce only a tetrameric uranyl(v) cluster. Interestingly, while for $(Np^{VI}O_2Cl_2)[Np^{V}O_2Cl(THF)_3]_2$ the cation–cation interactions necessarily occur between neptunium ions, the wheel complex is assembled in such a fashion that cation–cation interactions occur only between uranyl(v) units and Mn^{II} centers; individual uranyl(v) units are connected only *via* salen linkages. Static magnetic susceptibility data collected below 7 T revealed a sharp rise in $\chi_M T$ below ~ 60 K, similar to the susceptibility behavior observed for $(Np^{VI}O_2Cl_2)[Np^{V}O_2Cl(THF)_3]_2$. For the wheel complex, the behavior was also attributed to a combination of ligand field effects and coupling between metal centers; however, no modelling of the magnetic data was attempted due to the complexity of the system.

In addition to evidence of superexchange, blocking of the magnetization was observed for the $U_{12}Mn_6$ cluster in the form of magnetic hysteresis below 4.5 K. A drop in the magnetization at zero field occurs for all reported temperatures and is most pronounced at the lowest temperature of 2.25 K, indicative of quantum tunnelling of the magnetization. On the ac time-scale, slow magnetic relaxation was observed between 5 and 10 K under zero dc field and a 10 Oe oscillating field. The resulting relaxation times could be fit well to an Arrhenius law to give $U_{\text{eff}} = 99 \text{ cm}^{-1}$ with $\tau_0 = 3 \times 10^{-12} \text{ s}$. As the authors alluded to, diamagnetic substitution of the Mn^{II} centers within the wheel with Cd^{II} or Zn^{II} would provide valuable insight into the exact nature and origins of the magnetic coup-

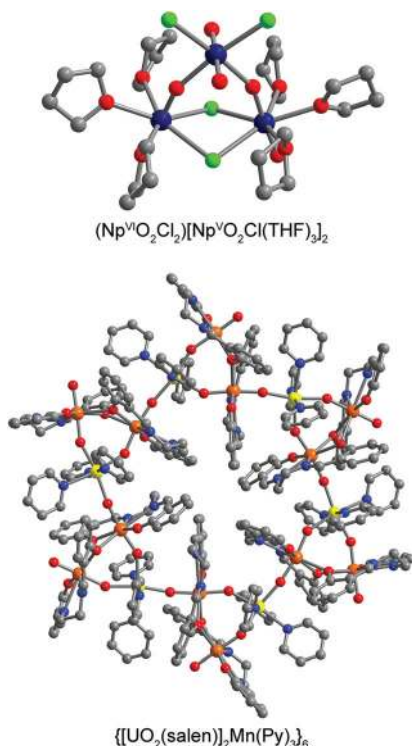


Fig. 7 Molecular structure of the neptunium cluster $(Np^{VI}O_2Cl_2)[Np^{V}O_2Cl(THF)_3]_2$ (top) and uranyl(v) wheel $\{[UO_2(salen)]_2Mn(Py)_3\}_6$ (bottom). Dark blue, orange, yellow, green, red, blue, and grey spheres represent Np, U, Mn, Cl, O, N, and C atoms, respectively; H atoms are omitted for clarity.^{9,58a}

ling. In addition, such an experiment would be an interesting probe of how the exchange coupling influences the observed slow magnetic relaxation.

Gratifyingly, it was found that by employing the same synthetic conditions but combining $[\text{Cp}^*\text{Co}][\text{UO}_2(\text{salen})(\text{Py})]$ and $\text{Mn}(\text{NO}_3)_2$ in a 1 : 1 ratio, the first actinide-based single-chain magnet could be isolated, namely $[\text{UO}_2(\text{salen})(\text{Py})][\text{Mn}(\text{Py})_4(\text{NO}_3)]$.^{58b} While this compound does not qualify as a single-molecule magnet, its magnetic behavior is noteworthy and further illustrative of the utility of exchange in actinide systems. Indeed, below a temperature of 150 K, dc magnetic susceptibility data exhibit a sharp rise in χ_{MT} , indicative of ferromagnetic coupling between the U^{V} and Mn^{II} centers. Moreover, ac susceptibility measurements under zero dc field revealed strong temperature and frequency dependence in the out-of-phase signal, χ_{M}'' , indicative of single-chain magnet behavior. This result was further supported by the observation of a linear regime in $\ln(\chi_{\text{MT}})$ versus $1/T$. In addition to a large relaxation barrier of $U_{\text{eff}} = 93 \text{ cm}^{-1}$, an open magnetic hysteresis loop was observed for this compound as high as 3 K. Interestingly, the analogous Cd^{II} -containing chain was also found to show slow relaxation of the magnetization (under an applied dc field), undoubtedly due to the single-ion anisotropy associated with the U^{V} centers. As expected, the relaxation was significantly faster and less temperature-dependent than observed for the UMn chain compound, although this result highlights the future utility of dominant axial ligand fields in mononuclear actinide complexes, as already demonstrated in the complex $\text{UO}(\text{Tren}^{\text{TIPS}})$. Indeed, mononuclear uranyl(v) complexes with weak equatorial ligands may present a worthwhile avenue for pursuit.

As the above examples demonstrate, exchange coupling is a promising route in the design of actinide single-molecule magnets with higher blocking temperatures. Given the ambiguous role of magnetic coupling in the slow magnetic relaxation in the foregoing molecular species, future design of exchange-coupled molecules might benefit from a view towards smaller nuclearity clusters, for which diamagnetic substitution can be more readily performed. Additionally, as the use of paramagnetic bridging ligands in dinuclear lanthanide complexes has proven the most successful route for exchange-coupled single-molecule magnets, a natural progression is the pursuit of analogous systems with actinide elements. While the N_2^{3-} radical is rather challenging synthetically, linkers such as bipyrimidine,^{6c} pyrazine,⁶⁰ and phenazine⁶¹ stand as more stable paramagnetic bridging species. As an example of the design of such structures, the mononuclear species $[\text{UTp}^{\text{Me}_2}_2(\text{bipy})]\text{I}$ stands as a useful building unit. Indeed, exchange of the bipyridine with bipyrimidine or other bridging N-heterocycles should facilitate the formation of a dinuclear complex that could be further reduced to form a radical-bridged species. The design and study of such simpler exchange-coupled structures holds immense promise, not only in extending the number of exchange-coupled actinide systems, but expanding our understanding of their unusual magnetic behavior.

Conclusions

Despite its late entrance into the field, actinide single-molecule magnetism is proving to be a richly varied and complex area of research. A key step forward will be the more rigorous characterization of relaxation dynamics in low-nuclearity species, including *via* dilution measurements, and particularly when a complex shows markedly different relaxation behavior depending on the applied magnetic field and/or temperature. Potentially promising mononuclear systems might be those with significantly higher axial site symmetries that may minimize state mixing and maximize orbital angular momentum. However, given the new challenges introduced with the use of the actinides, such as enhanced covalency and reactivity, it stands to reason that mononuclear complexes of these ions may be hard-pressed to succeed in the same way as their 4f forerunners. On the other hand, the few exchange-coupled systems studied suggest that rationally-designed multinuclear complexes may be a more direct route to successful single-molecule magnets with the actinides. The study of many more exchange-coupled systems is no doubt necessary to test this supposition. While no clear correlation currently exists thus far between superexchange and resulting magnetic properties, it is likely that strong exchange may help to shut down tunneling under zero applied field, thereby enabling slow magnetic relaxation. Even stronger magnetic exchange could potentially be facilitated through the use of radical bridging ligands. Undoubtedly progress in this area of research will require chemists and physicists to tackle new and difficult challenges in synthesis and characterization. Such efforts hold the promise of establishing a deeper understanding of actinide-based molecular magnetism.

Acknowledgements

The authors gratefully acknowledge support from the National Science Foundation under Grant CHE-1111900.

Notes and references

- (a) A. Caneschi, D. Gatteschi and R. Sessoli, *J. Am. Chem. Soc.*, 1991, **113**, 5873; (b) R. Sessoli, H.-L. Tsai, A. R. Schake, S. Wang, J. B. Vincent, K. Folting, D. Gatteschi, G. Christou and D. N. Hendrickson, *J. Am. Chem. Soc.*, 1993, **115**, 1804; (c) R. Sessoli, D. Gatteschi, A. Caneschi and M. A. Novak, *Nature*, 1993, **365**, 141.
- (a) N. Ishikawa, M. Sugita, T. Ishikawa, S.-y. Koshihara and Y. J. Kaizu, *J. Am. Chem. Soc.*, 2003, **125**, 8694; (b) N. Ishikawa, M. Sugita, T. Ishikawa, S.-Y. Koshihara and Y. Kaizu, *J. Phys. Chem. B*, 2004, **108**, 11265.
- (a) J.-L. Liu, Y.-C. Chen, Y.-Z. Zheng, W.-Q. Lin, L. Ungur, W. Wernsdorfer, L. F. Chibotaru and M.-L. Tong, *Chem. Sci.*, 2013, **4**, 3310; (b) K. R. Meihaus and J. R. Long, *J. Am. Chem. Soc.*, 2013, **135**, 17952; (c) L. Ungur, J. J. Le Roy,

- I. Korobkov, M. Murugesu and L. F. Chibotaru, *Angew. Chem., Int. Ed.*, 2014, **53**, 4413; (d) J. J. Le Roy, L. Ungur, I. Korobkov, L. F. Chibotaru and M. Murugesu, *J. Am. Chem. Soc.*, 2014, **136**, 8003.
- 4 (a) J. M. Zadrozny, M. Atanasov, A. M. Bryan, C.-Y. Lin, B. D. Rekker, P. P. Power, F. Neese and J. R. Long, *Chem. Sci.*, 2013, **4**, 139; (b) J. M. Zadrozny, D. J. Xiao, M. Atansov, G. J. Long, F. Grandjean, F. Neese and J. R. Long, *Nat. Chem.*, 2013, **5**, 577.
- 5 I.-R. Jeon, J. G. Park, D. J. Xiao and T. D. Harris, *J. Am. Chem. Soc.*, 2013, **135**, 16845.
- 6 (a) J. D. Rinehart, M. Fang, W. Evans and J. R. Long, *Nat. Chem.*, 2011, **3**, 538; (b) J. D. Rinehart, M. Fang, W. Evans and J. R. Long, *J. Am. Chem. Soc.*, 2011, **133**, 14236; (c) S. Demir, J. M. Zadrozny, M. Nippe and J. R. Long, *J. Am. Chem. Soc.*, 2012, **134**, 18546.
- 7 N. Edelstein, *J. Alloys Compd.*, 1995, **223**, 197.
- 8 H. M. Crosswhite, H. Crosswhite, W. T. Carnall and A. P. Paszek, *J. Chem. Phys.*, 1980, **72**, 5103.
- 9 N. Magnani, E. Colineau, R. Eloirdi, J.-C. Griveau, R. Caciuffo, S. M. Cornet, I. May, C. A. Sharrad, D. Collison and R. E. P. Winpenny, *Phys. Rev. Lett.*, 2010, **104**, 197202.
- 10 D. N. Woodruff, R. E. P. Winpenny and R. A. Layfield, *Chem. Rev.*, 2013, **113**, 5110.
- 11 R. A. Layfield, *Organometallics*, 2014, **33**, 1084.
- 12 (a) N. Magnani, *Int. J. Quantum Chem.*, 2014, **114**, 755; (b) Also see D. R. Kindra and W. J. Evans, *Chem. Rev.*, 2014, **114**, 8865 for a comprehensive review on the variability of magnetic susceptibility in U^{III} , U^{IV} , and U^V complexes.
- 13 (a) J. D. Rinehart and J. R. Long, *Chem. Sci.*, 2011, **2**, 2078; (b) N. F. Chilton, S. K. Langley, B. Moubarak, A. Soncini, S. R. Batten and K. S. Murray, *Chem. Sci.*, 2013, **4**, 1719; (c) J. J. Le Roy, I. Korobkov and M. Murugesu, *Chem. Commun.*, 2014, **50**, 1602. This is of course only one first step in a possible route to accessing systems showing slow relaxation and large relaxation barriers. Additional factors such as large axial anisotropy and nearly collinear ground and first excited state anisotropy axes have been shown to promote slow relaxation through thermally activated means. However, these attributes are often only determined computationally, after synthesis and ac susceptibility characterization, in order to further rationalize observed magnetic relaxation behavior.
- 14 The potential for covalency poses an additional challenge in the theoretical description of actinide-based complexes that is not an issue for the lanthanides. Alternatively, stronger metal–ligand interactions may aid in more fine-tuning of the electronics and therefore magnetic relaxation than is possible with the lanthanides.
- 15 (a) H. Reddmann, C. Apostolidis, O. Walter and H.-D. Amberger, *Z. Anorg. Allg. Chem.*, 2006, **632**, 1405; (b) C. Apostolidis, A. Morgenstern, J. Rebizant, B. Kanellakopoulos, O. Walter, B. Powietzka, M. Karbowiak, H. Reddmann and H.-D. Amberger, *Z. Anorg. Allg. Chem.*, 2010, **636**, 201.
- 16 The spin–orbit coupling constant ζ_{nf} is a coefficient used to describe the magnitude of the interaction between the spin magnetic moment of an individual electron with the magnetic field generated by its motion around the nucleus; the crystal field parameters B_q^k are obtained from transformation of corresponding coefficients within the crystal field Hamiltonian, where $k = 1 \dots 7$ and $q = 0 \dots 6$ increasing in integer values, see C. Görller-Walrand and K. Binnemans, *Handbook of the Physics and Chemistry of the Rare Earths*, ed. K. A. Gschneidner Jr. and L. Eyrin, Elsevier, Amsterdam, 1996, Vol. 23, pp. 121–283. The sign and magnitude of B_0^2 is relevant as it influences the sign and magnitude of the magnetic anisotropy, see ref. 17. $N_{\nu}/\sqrt{4\pi}$ of course represents the strength of the crystal field experienced by U^{3+} or Nd^{3+} due to the perturbation of the nf electrons by those of the Cl^- or $[Tp]^-$ (tris(pyrazolyl)borate anion) ligands.
- 17 (a) A. Szytuła and J. Leciejewicz, *Handbook of Crystal Structures and Magnetic Properties of Rare Earth Intermetallics*, CRC Press, Boca Raton, Florida, 1994; (b) R. Skomski, *Simple Models of Magnetism*, Oxford University Press, Oxford, 2008.
- 18 (a) M. R. MacDonald, M. E. Fieser, J. E. Bates, J. W. Ziller, F. Furche and W. J. Evans, *J. Am. Chem. Soc.*, 2013, **135**, 13310; (b) H. S. La Pierre, A. Scheurer, F. W. Heinemann, W. Hieringer and K. Meyer, *Angew. Chem., Int. Ed.*, 2014, **53**, 7158.
- 19 J. D. Rinehart and J. R. Long, *J. Am. Chem. Soc.*, 2009, **131**, 12558.
- 20 L. Maria, M. P. Campello, Â. Domingos, I. Santos and R. Andersen, *J. Chem. Soc., Dalton Trans.*, 1999, 2015.
- 21 Y. Sun, J. Takats, T. Eberspacher and V. Day, *Inorg. Chim. Acta*, 1995, **229**, 315.
- 22 J. D. Rinehart, K. R. Meihaus and J. R. Long, *J. Am. Chem. Soc.*, 2010, **132**, 7572.
- 23 K. R. Meihaus, J. D. Rinehart and J. R. Long, *Inorg. Chem.*, 2011, **50**, 8484.
- 24 J. J. Baldoví, S. Cardona-Serra, J. M. Clemente-Juan, E. Coronado and A. Gaita-Ariño, *Chem. Sci.*, 2013, **4**, 938. This corrected model was used to improve previous approaches that treat the ligands as point charges and therefore does not account for potential overlap and covalency.
- 25 J. D. Rinehart and J. R. Long, *Dalton Trans.*, 2012, **41**, 13572.
- 26 K. R. Meihaus, S. G. Minasian, W. W. Lukens, Jr., S. A. Kozimor, D. K. Shuh, T. Tylliszczak and J. R. Long, *J. Am. Chem. Soc.*, 2014, **136**, 6056.
- 27 M. A. Antunes, L. C. J. Pereira, I. C. Santos, M. Mazzanti, J. Marçalo and M. Almeida, *Inorg. Chem.*, 2011, **50**, 9915.
- 28 J. T. Coutinho, M. A. Antunes, L. C. J. Pereira, H. Bolvin, J. Marçalo, M. Mazzanti and M. Almeida, *Dalton Trans.*, 2012, **41**, 13568.
- 29 It should be mentioned here that the same authors recently reported the very interesting result that $UTp^{Me_2}_2I$ can actually form three different structures depending on the crystallization conditions (see (a) M. A. Antunes, I. C. Santos,

- H. Bolvin, L. C. J. Pereira, M. Mazzanti, J. Marçalo and M. Almeida, *Dalton Trans.*, 2013, **42**, 8861 and (b) Y. M. Sun, R. McDonald, J. Takats, V. W. Day and T. A. Eberspacher, *Inorg. Chem.*, 1994, **33**, 4433). Two of these structures involve an inner-sphere iodide ligand, while the third is a high symmetry structure wherein the iodide is outer-sphere and shortening of the U–N bond lengths is concomitant with a decrease in crowding around the uranium center. Crystal field modelling of the magnetic data for this compound by Baldoví *et al.* (ref. 24) was performed using the originally reported structure by Takats *et al.* with an inner-sphere iodide. However, as reported in ref. 29a, powder diffraction data support that the reported magnetism corresponds with the high symmetry cationic form $[\text{UTp}^{\text{Me}_2}_2]\text{I}$. While *ab initio* computations on all three structures reveal differences in the separation between ground and first excited M_J states for each complex, nonetheless these values compare well with ref. 7, are all the same order of magnitude, and significantly larger than the experimentally determined barrier of 21.0 cm^{-1} .
- 30 S. J. Kraft, P. E. Fanwick and S. C. Bart, *Inorg. Chem.*, 2010, **49**, 1103.
- 31 J. T. Coutinho, M. A. Antunes, L. C. J. Pereira, J. Marçalo and M. Almeida, *Chem. Commun.*, 2014, **50**, 10262.
- 32 F. Moro, D. P. Mills, S. T. Liddle and J. Van Slageren, *Angew. Chem., Int. Ed.*, 2013, **52**, 3430.
- 33 D. P. Mills, F. Moro, J. McMaster, J. van Slageren, W. Lewis, A. J. Blake and S. T. Liddle, *Nat. Chem.*, 2011, **3**, 454.
- 34 D. M. King, F. Tuna, J. McMaster, W. Lewis, A. J. Blake, E. J. L. McInnes and S. T. Liddle, *Angew. Chem., Int. Ed.*, 2013, **52**, 4921.
- 35 N. Magnani, C. Apostolidis, A. Morgenstern, E. Colineau, J.-C. Griveau, H. Bolvin, O. Walter and R. Caciuffo, *Angew. Chem., Int. Ed.*, 2011, **50**, 1696.
- 36 D. Karraker, J. A. Stone, E. R. Jones, Jr. and N. Edelstein, *J. Am. Chem. Soc.*, 1970, **92**, 4841.
- 37 One additional low-nuclearity system not mentioned above is the molecule $[\text{UO}_2\text{Dy}(\text{py})_2(\text{L})_2]_2$ (L = Pacman ligand) from ref. 57b, which was found to show a butterfly-shaped magnetic hysteresis loop at 3 K. The authors attributed the observed slow relaxation of the magnetization to Dy^{III} single-ion anisotropy, thus it is not included under the category of actinide single-molecule magnets here, where slow relaxation is inherently assumed to arise predominantly from the actinide metal center(s).
- 38 N. Magnani, E. Colineau, J.-C. Griveau, C. Apostolidis, O. Walter and R. Caciuffo, *Chem. Commun.*, 2014, **50**, 8171.
- 39 For example ref. 13a; in some cases, the measured energy barrier corresponds to relaxation via higher excited states if level crossing is not allowed from the first excited state, for instance ref 3c and (a) R. J. Blagg, L. Ungur, F. Tuna, J. Speak, P. Comar, D. Collison, W. Wernsdorfer, E. J. L. McInnes, L. F. Chibotaru and R. E. P. Winpenny, *Nat. Chem.*, 2013, **5**, 673. It should also be noted, however, that while correlations between M_J separations and U_{eff} have been observed for lanthanide complexes, this is not always the case, and again it is important to consider alternative spin-lattice relaxation processes, for example see (b) K. S. Pedersen, L. Ungur, M. Sigríst, A. Sundt, M. Schau-Magnussen, V. Vieru, H. Mutka, S. Rols, H. Weihe, O. Waldmann, L. F. Chibotaru, J. Bendix and J. Dreiser, *Chem. Sci.*, 2014, **5**, 1650. As is noted in the latter reference, a given ac frequency and temperature range may limit the observation of Orbach relaxation, and this process should not be taken for granted in mononuclear systems.
- 40 The exponent n ranges most commonly from 5–9, with values of 8 or 9 typically corresponding with Kramers ions such as U^{III} .
- 41 Another point to briefly touch on here is the assumption of idealized symmetry both in crystal field models and in the simulation of EPR data. This protocol is useful in obtaining a model, but also can be less directly informative when the actual molecular symmetry is significantly lower (as in the case of $[\text{UTp}^{\text{Me}_2}_2(\text{bipy})]\text{I}$ and $[\text{UTp}^{\text{Me}_2}_2]\text{I}$, modelled with D_{5h} symmetry). In the absence of computations, it is also important that careful consideration of experimental and literature data be considered before making claims regarding properties such as magnetic ground state. Consider for example the case of C_{3v} symmetric complex $\text{UO}(\text{Tren}^{\text{TIPS}})$. Based on the absence of an EPR signal for this complex and experimental magnetization data, the authors assume a pure $M_J = \pm 3/2$ ground state. For a pure ground state though, it is hard to rationalize tunnelling of the magnetization at zero field since, if dipolar interactions are null, then there is no other mechanism by which tunnelling should be expected to arise in a Kramers system with a pure ground state. However, isoelectronic CeIII has been studied in C_{3v} symmetry, and the ground M_J doublet is not pure, and further it does not contain any contribution from $M_J = \pm 3/2$. Thus, there is likely more complexity to the magnetization dynamics in $\text{UO}(\text{Tren}^{\text{TIPS}})$ than first appears.
- 42 Demonstrated through EPR for $\text{U}(\text{Bc}^{\text{Me}})_3$ and $\text{U}(\text{Bp}^{\text{Me}})_3$ and computationally for the other complexes.
- 43 This is reasonable given the trigonal prismatic geometry around the uranium center in these complexes; only UTp_3 possesses crystallographically-imposed D_{3h} symmetry.
- 44 A. Abragam and B. Bleaney, *Electron Paramagnetic Resonance of Transition Ions*, Clarendon Press, Oxford, 1970.
- 45 Another interesting consideration is the design of low-coordinate, high site symmetry complexes with low crystal symmetry. Ref. 13b presents calculations on the internal fields experienced by Dy^{III} centers in mononuclear β -diketonate complexes. Due to the greater number of symmetry operations and therefore molecular orientations in $P2_1/c$ versus $P\bar{1}$, a single Dy^{III} center in the former complex experiences two different internal fields, whereas for the $P\bar{1}$ symmetry, only one type of internal field is present.
- 46 If χ_{T} is more than χ_{dc} , this of course indicates a calculation error, as the in-phase susceptibility can never exceed the total magnetic susceptibility for the molecule. Unfortunately, for many of the literature compounds, comparison

- of χ_T to χ_{dc} at the same temperature revealed calculation errors in over half of the complexes, strongly suggesting a need for more careful workup and also analysis of experimental data.
- 47 D. Gatteschi, R. Sessoli and J. Villain, *Molecular Nanomagnets*, Oxford University Press, Oxford, 2006.
- 48 In re-plotting the Arrhenius data for Fig. 5 from ref. 11, we obtained a U_{eff} value of 21.2 cm^{-1} from fitting the highest four temperatures to an Arrhenius law. However, the corresponding τ_0 value was found to be $4.3 \times 10^{-8} \text{ s}$, rather than the reported $\tau_0 = 1.8 \times 10^{-7} \text{ s}$. Therefore, this former value is deemed more accurate and is the value represented in the solid blue line in Fig. 5 and also that used to determine the corresponding 2 K relaxation time. Even using the Arrhenius parameters exactly as reported, the relaxation time at 2 K is $\sim 0.7 \text{ s}$, very rapid for the observation of magnetic hysteresis.
- 49 As long as systems continue to be measured under an applied field, and given the hysteresis ambiguity, one further important measurement would be determination of the relaxation time at various fields and the magnetic hysteresis temperature. Accompanied with the same measurement performed on a highly diluted sample, this would provide strong evidence that the magnetic hysteresis is indeed molecular in origin.
- 50 R. K. Rosen, R. A. Andersen and N. M. Edelstein, *J. Am. Chem. Soc.*, 1990, **112**, 4588.
- 51 J. D. Rinehart, T. D. Harris, S. A. Kozimor, B. M. Bartlett and J. R. Long, *Inorg. Chem.*, 2009, **48**, 3382 and references therein.
- 52 W. W. Lukens and M. D. Walter, *Inorg. Chem.*, 2010, **49**, 4458.
- 53 J. D. Rinehart, B. M. Bartlett, S. A. Kozimor and J. R. Long, *Inorg. Chim. Acta*, 2008, **361**, 3534.
- 54 D. Patel, F. Moro, J. McMaster, W. Lewis, A. J. Blake and S. T. Liddle, *Angew. Chem., Int. Ed.*, 2011, **50**, 10388.
- 55 F. Habib and M. Murugesu, *Chem. Soc. Rev.*, 2013, **42**, 3278 and references therein.
- 56 W. W. Lukens, N. Magnani and C. H. Booth, *Inorg. Chem.*, 2012, **51**, 10105.
- 57 (a) L. Chatelain, V. Mougel, J. Pécaut and M. Mazzanti, *Chem. Sci.*, 2012, **3**, 1075; (b) P. L. Arnold, G. M. Jones, S. O. Odoh, G. Schreckenbach, N. Magnani and J. B. Love, *Nat. Chem.*, 2012, **4**, 221.
- 58 (a) V. Mougel, L. Chatelain, J. Pécaut, R. Caciuffo, E. Colineau, J.-C. Griveau and M. Mazzanti, *Nat. Chem.*, 2012, **4**, 1101; (b) V. Mougel, L. Chatelain, J. Hermle, R. Caciuffo, E. Colineau, F. Tuna, N. Magnani, A. De Geyer, J. Pécaut and M. Mazzanti, *Angew. Chem., Int. Ed.*, 2014, **53**, 819.
- 59 (a) P. L. Arnold, E. Hollis, F. J. White, N. Magnani, R. Caciuffo and J. B. Love, *Angew. Chem., Int. Ed.*, 2011, **50**, 887; (b) P. L. Arnold, E. Hollis, G. S. Nichol, J. B. Love, J.-C. Griveau, R. Caciuffo, N. Magnani, L. Maron, L. Castro, A. Yahia, S. O. Odoh and G. Schreckenbach, *J. Am. Chem. Soc.*, 2013, **135**, 3841.
- 60 T. Mehdoui, J.-C. Berthet, P. Thuéry and M. Ephritikhine, *Eur. J. Inorg. Chem.*, 2004, 1996.
- 61 W. J. Evans, M. K. Takase, J. W. Ziller, A. G. DiPasquale and A. L. Rheingold, *Organometallics*, 2009, **28**, 236.